Int J Appl Earth Obs Geoinformation 62 (2017) 144–156

Contents lists available at ScienceDirect

Int J Appl Earth Obs Geoinformation

journal homepage: www.elsevier.com/locate/jag

Automated delineation and characterization of drumlins using a localized contour tree approach

Shujie Wang[a], Qiusheng Wu[b,*], Dylan Ward[c]

[a] Department of Geography & Geographic Information Science, University of Cincinnati, Cincinnati, OH, USA
[b] Department of Geography, Binghamton University, State University of New York, Binghamton, New York, USA
[c] Department of Geology, University of Cincinnati, Cincinnati, OH, USA

ARTICLE INFO

Keywords:
Drumlin
Contour tree
LiDAR
Morphology
Spatial pattern

ABSTRACT

Drumlins are ubiquitous landforms in previously glaciated regions, formed through a series of complex subglacial processes operating underneath the paleo-ice sheets. Accurate delineation and characterization of drumlins are essential for understanding the formation mechanism of drumlins as well as the flow behaviors and basal conditions of paleo-ice sheets. Automated mapping of drumlins is particularly important for examining the distribution patterns of drumlins across large spatial scales. This paper presents an automated vector-based approach to mapping drumlins from high-resolution light detection and ranging (LiDAR) data. The rationale is to extract a set of concentric contours by building localized contour trees and establishing topological relationships. This automated method can overcome the shortcomings of previously manual and automated methods for mapping drumlins, for instance, the azimuthal biases during the generation of shaded relief images. A case study was carried out over a portion of the New York Drumlin Field. Overall 1181 drumlins were identified from the LiDAR-derived DEM across the study region, which had been underestimated in previous literature. The delineation results were visually and statistically compared to the manual digitization results. The morphology of drumlins was characterized by quantifying the length, width, elongation ratio, height, area, and volume. Statistical and spatial analyses were conducted to examine the distribution pattern and spatial variability of drumlin size and form. The drumlins and the morphologic characteristics exhibit significant spatial clustering rather than randomly distributed patterns. The form of drumlins varies from ovoid to spindle shapes towards the downstream direction of paleo ice flows, along with the decrease in width, area, and volume. This observation is in line with previous studies, which may be explained by the variations in sediment thickness and/or the velocity increases of ice flows towards ice front.

1. Introduction

Drumlins are elongate oval-shaped hills with a long axis oriented parallel to the ice flow direction and a stoss face that is generally steeper than the lee face (Benn and Evans 2014; Menzies, 1979). They typically occur as swarms or large groups in the previously glaciated regions, formed through the complex interactions between the substrates, flowing ice and subglacial meltwater (Kerr and Eyles, 2007; Shaw, 1989; Shaw and Freschauf, 1973). Numerous drumlins have been identified in North America as the products of the subglacial processes beneath the Laurentide Ice Sheet during the Wisconsin glaciation (Kerr and Eyles, 2007; Maclachlan and Eyles, 2013). The form and composition of drumlins preserve crucial information regarding the dynamic behaviors of paleo-ice sheets and the subglacial processes beneath the ice sheets (Boulton and Clark, 1990; Kleman and Borgström, 1996). Besides their alignment with former ice flow directions, the elongation ratio of drumlins has been suggested to be related to previous ice velocities (Briner, 2007; Hart, 1999; Hess and Briner, 2009). Accurate and detailed mapping of drumlins is therefore fundamentally important for reconstructing the evolving processes of past glaciations. The morphology of drumlins provides information about changes in the subglacial environments over time and space (Knight, 1997). Length, width, height, volume, orientation, and elongation ratio are commonly used to describe the morphological characteristics of drumlins (Clark et al., 2009; Spagnolo et al., 2012). Quantitative characterization of the size and shape properties of drumlins and the spatial variation patterns of these morphological metrics may give insights into the formation processes of drumlins (Hindmarsh, 1999; Pelletier, 2008

Traditionally, drumlins were mapped through fieldwork measurement (Rose and Letzer, 1977) and manual digitization from topographic

* Corresponding author.
E-mail addresses: wang2sj@mail.uc.edu (S. Wang), wqs@binghamton.edu (Q. Wu), warddy@ucmail.uc.edu (D. Ward).

http://dx.doi.org/10.1016/j.jag.2017.06.006
Received 3 May 2017; Received in revised form 13 June 2017; Accepted 14 June 2017

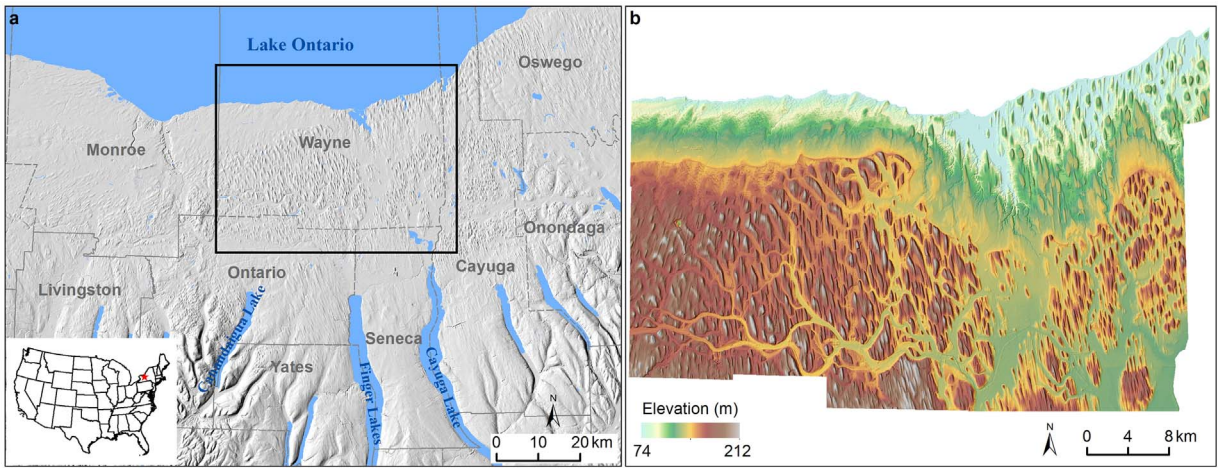

Fig. 1. (a) Study area and (b) LiDAR DEM data.

maps (Rose and Letzer, 1977), aerial photographs (Clark, 1993; Shaw, 1983), satellite images (Clark, 1994; Clark and Stokes, 2001; Jansson and Glasser, 2005; McCABE et al., 1999; Stokes, 2002), and digital elevation model (DEM) visualizations (Hughes et al., 2010; Livingstone et al., 2008; Smith et al., 2009; Smith and Clark, 2005). The practicability and accuracy of these methods are limited by several disadvantages. Field mapping is time-consuming and costly. Manual digitization may introduce human errors when the drumlin edges are camouflaged by land cover on aerial photographs or satellite images (Saha et al., 2011). The DEM visualization based methods are affected by the different illumination settings and visualization enhancement techniques (Hughes et al., 2010; Smith and Clark, 2005). The recent development of object-oriented approaches has enabled the automated extraction of various landforms, such as alluvial fans (Argialas and Tzotsos, 2006), landslides (Lu et al., 2011; Martha et al., 2010), and drumlins (d'Oleire-Oltmanns et al., 2013; Saha et al., 2011). The object-oriented analysis is based on segmented irregular objects rather than individual pixels. Land-surface segmentation approaches (d'Oleire-Oltmanns et al., 2013; Eisank et al., 2014; Evans, 2012; Saha et al., 2011) have been developed to delineate drumlins by subdividing a DEM into morphologically homogeneous terrain segments based on a set of surface parameters (e.g., slope, aspect, and curvature). Saha et al., 2011Saha et al. (2011) applied the multiresolution segmentation approach to partition a USGS 30-m resolution DEM into irregularly shaped regions at multiple scales, and extracted the drumlins in the Chautauqua drumlin field using a rule-based classification scheme. Eisank et al. (2014) assessed the multiresolution segmentation algorithm using different parameter settings for drumlin delineation from synthetic DEMs. The accuracy and efficiency of the land-surface segmentation methods are affected by various factors, including the segmentation algorithm, the segmentation parameters (e.g., scale), the land-surface parameters, and the training samples used for drumlin identification. This object-oriented framework also has limitations when applied to high-resolution DEMs by increasing the computational complexity of segmentation and producing errors due to the high frequency noise of high-resolution topographic data (Esri, 2016).

The advent of airborne light detection and ranging (LiDAR) technologies has generated large volumes of highly accurate and densely sampled surface elevation measurements with a spatial resolution of 1–5 m for rasterized DEMs. The significantly improved spatial resolution of the DEMs from LiDAR systems has allowed the delineation and analysis of geomorphological features at finer scales (Brubaker et al., 2013; Hodge et al., 2009; Notebaert et al., 2009) in comparison with the traditional moderate resolution DEMs. To fully exploit the greater spatial details of high-resolution DEMs for drumlin characterization and overcome the shortcomings of land-surface segmentation approach, this research employed a localized contour tree framework (Wu et al., 2015) to delineate the drumlins and quantify their morphological properties. Wu et al. (2015) designed the graph theory-based localized contour tree method to automatically derive geometric and topological properties of surface depressions from high-resolution topographic data. This automated algorithm imitates the reasoning process of a human interpreter to visually recognize surface depressions from a topographic map. By analogy with the surface depression that is a sunken area on Earth's surface surrounded by higher ground in all directions, an individual drumlin is a raised area surrounded by lower ground in all directions. This paper aims to adapt the localized contour tree method and develop an automated framework to delineate drumlins from high-resolution LiDAR data. We applied the proposed method to extract the drumlins over a study area within the New York Drumlin Field, USA. The accuracy of the automated method was assessed by comparing with the manual digitization method. Based on the drumlin extraction results, we quantified the morphological characteristics of drumlins and analyzed the statistical and spatial distribution patterns.

2. Study area and datasets

The case study area (Fig. 1(a)) is a portion of the New York Drumlin field between the south shore of Lake Ontario and Cayuga Lake. The total area is 2200 km^2. The sedimentary bedrock of this region is susceptible to erosion, thus being relatively flat and low in elevation. The New York Drumlin Field was last glaciated about 18,000 years ago (Kerr and Eyles, 2007), where the southern lobes of the Laurentide Ice sheet flowed over. The southern lobes have been considered as the dynamic outlets of transporting large quantities of sediments and ice from the interior ice sheet to the periphery (Hess and Briner, 2009; Jennings, 2006). Briner (2007) used the morphological measurements of the New York Drumlin Field as the supporting evidence that elongate subglacial bedforms characterize fast ice flows. Sedimentological and geomorphic data suggest that these drumlins are the erosion products of preexisting sediments (Kerr and Eyles, 2007).

Massive LiDAR data have been collected for the New York State through many different projects. The GIS Program Office of the New York State Office of Information Technology Services (NYS ITS) releases high-resolution LiDAR-derived DEMs in collaboration with the Federal Emergency Management Agency (FEMA). We used the bare-earth LiDAR-derived DEMs in this study, including a 2-m FEMA DEM covering most of the study area and a 1-m FEMA DEM covering the northernmost coastal area. These DEMs are freely available on the NYS GIS Clearinghouse website. The 2-m FEMA DEM was generated by the LiDAR data acquired by a topographic LiDAR system during 2012–2014. The nominal point spacing is 1.5 m, and the horizontal and

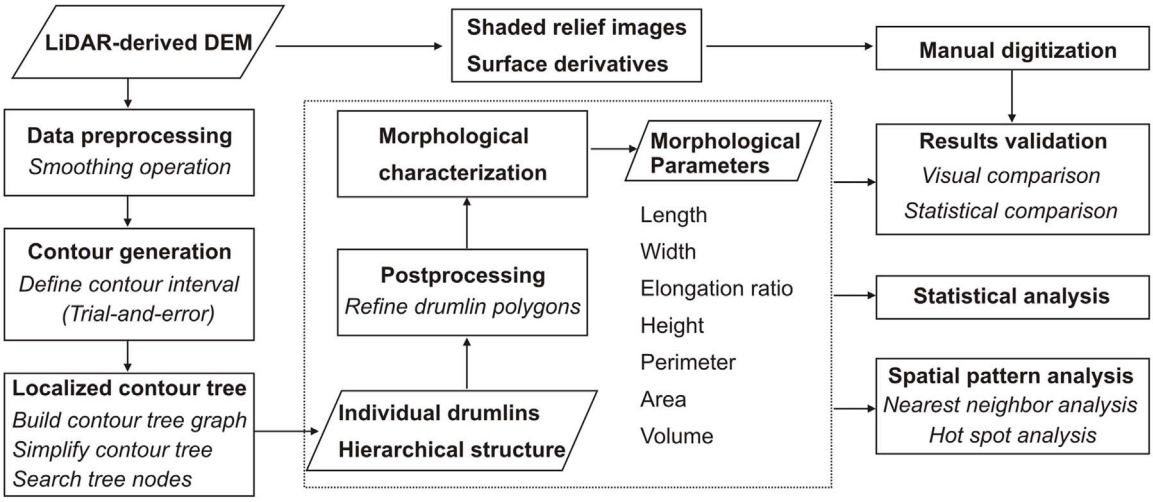

Fig. 2. Workflow diagram of drumlin delineation and characterization based on the localized contour tree method.

vertical accuracies are 3.21 m and 0.145 m at the 95% confidence level respectively (Seneca Watershed LiDAR Control, 2014). The 1-m FEMA DEM was created from the LiDAR data collected during 2014–2015 which have point spacing of 0.7 m, horizontal accuracy of 1 m and vertical accuracy of 3.3 cm RMSE (United States Interagency Elevation Inventory, 2016). The 1-m FEMA DEM was resampled to 2-m resolution using the bilinear resampling method and the generated LiDAR DEM mosaic is shown in Fig. 1(b).

3. Methods

As illustrated in Fig. 2, our methodology for delineating and characterizing drumlins consists of several key steps: (1) preprocessing of the LiDAR-derived DEM; (2) automated delineation of drumlins using the localized contour tree method; (3) quantification of the drumlin morphological properties; (4) refinement of the drumlin polygons; (5) validation of the extracted drumlins; and (6) characterization of the spatial variation patterns of drumlins.

3.1. Preprocessing of LiDAR data

Our method for automated delineation of drumlins is essentially a vector-based approach through identifying patterns of concentric contours. Since high-resolution LiDAR-derived DEMs tend to generate jagged or irregular contours due to random errors, it is a common practice to smooth LiDAR DEMs before using them for analysis (Li et al., 2011). One of the most commonly used filters for smoothing DEMs is the median filter (Liu et al., 2010; Wu et al., 2014), which is available in the ArcGIS Focal Statistics tool. More advanced filters can be found in other open-source GIS software packages, such as the Whitebox Geospatial Analysis Tools (GAT). The advanced filters available in the Whitebox GAT include the adaptive filter, Gaussian filter, K-Nearest mean filter, among others (Lindsay, 2016). In this study, we used a simple 3 × 3 median filter to smooth the LiDAR DEM and suppress data noise.

3.2. Automated delineation of drumlins

Based on the smoothed DEM, we generated contours using a 2-m contour interval. Two types of contours were generated: closed-loop contours and open contours. Open contours are those contours intersecting DEM edges without forming a closed loop. Since the basic assumption of our method is that a drumlin is represented by a set of concentric closed-loop contours on a contour map, we eliminated the open contours and only kept the closed-loop contours for further analysis. Then, we adopted and adapted the localized contour tree method (Wu et al., 2015) to delineate drumlins. The localized contour tree method was originally developed to identify and characterize the nested hierarchical structure of surface depressions. It has been successfully applied to identify depressional features from digital elevation data, such as wetland depressions (Wu and Lane, 2017, 2016) and sinkholes (Wu et al., 2016). The basic assumption of the localized contour tree method for identifying nested depressions from a contour map is that a topographic depression can be represented by a series of closed-loop contours in a concentric pattern with the outer contours having higher elevations than the inner contours (Wu et al., 2015). In contrast, we assumed that a drumlin on a contour map could be represented by a series of concentric closed-loop contours with the outer contours having lower elevations than the inner contours.

Drumlins may vary in size, height, and shape. In general, there are two types of drumlins: single drumlins and compound drumlins (also known as drumlin swarms in the literature). Single drumlins are simple isolated topographic highs, whereas compound drumlins are more complex with two or more single drumlins nested inside (Maclachlan and Eyles, 2013). On a contour map, a compound drumlin is manifested by a nested structure of multiple sets of concentric closed-loop contours with elevation values decreasing from inside to outside. Fig. 3 shows an example of a compound drumlin, which appears to have three single drumlins nested inside. To automate the process for identifying drumlins from a contour map using the localized contour tree method, the first key step is to identify the innermost contour of a drumlin, which is the closed-loop contour that does not enclose any other contours. As shown in Fig. 3(a), contours A, D, and G are the three innermost contours (see the red contours in Fig. 3(a)). Each innermost contour is the highest elevation contour for the corresponding single drumlin, respectively. Once the innermost contours are identified, they are pushed into a priority queue. The innermost contour with the highest elevation is given the highest priority, whereas the one with the lowest elevation is given the lowest priority. The algorithm then iterates the priority queue and starts searching outward for other associated closed-loop contours for each innermost contour. For example, since the innermost contour A (see Fig. 3(a)) has the highest elevation, it serves as the starting point to search outward for other associated concentric contours. In this case, contours B and C are the associated concentric contours for the innermost contour A. The outermost contour for this set of concentric contours is contour C, which is defined as the level-1 contour. Similarly, the outermost contours for the other two single drumlins are contours F and K, respectively (see the yellow contours in Fig. 3(a)). The three level-1 contours (C, F, and K), which indicate the spatial extent of the three single drumlins, serve as the starting point in

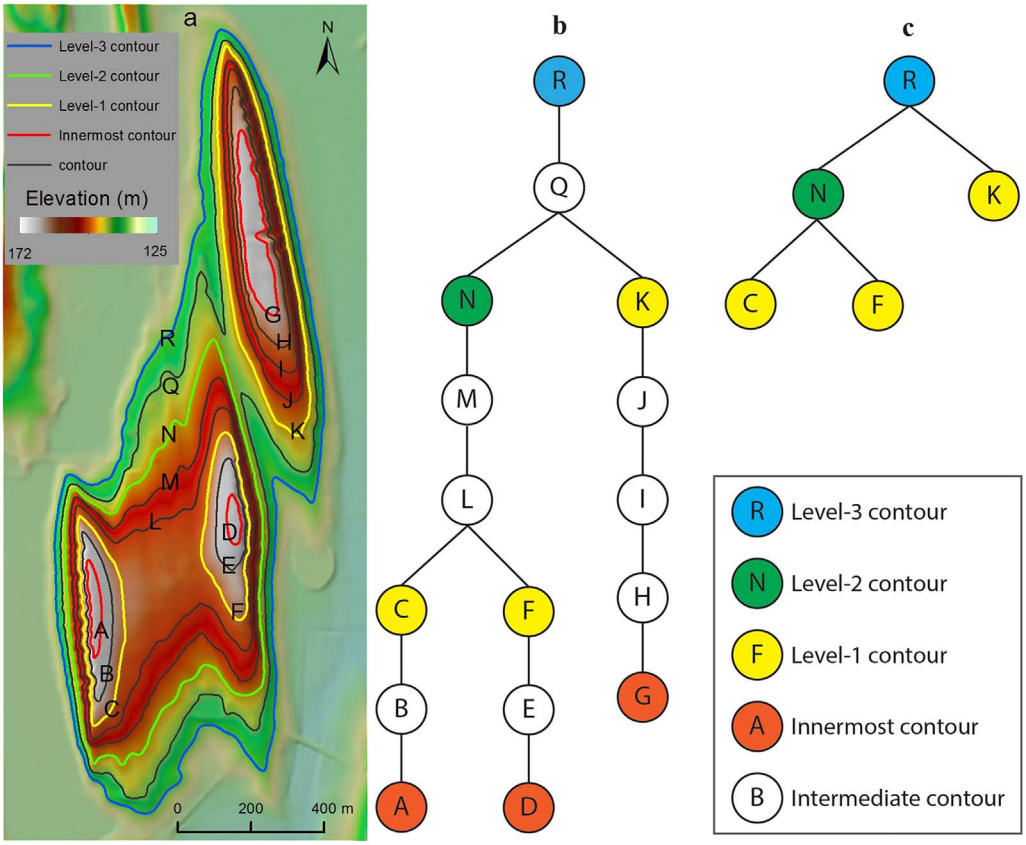

Fig. 3. A localized contour tree representation of a compound drumlin. (a) Contours with a 5-m contour interval overlaid on the shaded relief of a LiDAR DEM. (b) Contour tree graph of the compound drumlin shown in (a). (c) A simplified contour tree graph.

the next round for searching higher level contours. The outward neighboring contour of contour C is contour L, which also encloses contour F. When a contour encloses two or more level-1 contours, it becomes a level-2 contour. The search for level-2 contours continues until the outermost contour for this set of concentric contour is found (e.g., contour N in Fig. 3(a)). This iterative search continues until all contours are visited and their contour levels are determined accordingly. Whenever two drumlins merge, a higher-level drumlin is created.

The topological relationship between drumlins can be represented using a contour tree graph, which is composed of nodes and links. Each node corresponds to a contour, whereas each link indicates the adjacency and containment relationships between contours. Fig. 3(b) shows a corresponding contour tree representation of the compound drumlin shown in Fig. 3(a). The nested hierarchical structure of the compound drumlin can be clearly seen from the contour tree graph. The tree is built from bottom to top, starting from the three innermost contours and growing upward. The merging of two nodes indicates a change in the topological relationship, which results in a higher-level drumlin. The root node of the tree represents the outermost contour of the compound drumlin, i.e., the maximum spatial extent of the compound drumlin. The localized contour tree algorithm builds a set of trees for the entire area. Each tree represents one disjointed drumlin, which can either be a single or compound drumlin. A single drumlin constitutes a single-branch contour tree, whereas a compound drumlin constitutes a multi-branch contour tree.

As shown in Fig. 3(b), the multi-branch contour tree is composed of nodes representing critical contours with assigned levels as well as some intermediate contours. The number of nodes representing intermediate contours varies depending on the contour interval used for generating contours. The smaller the contour interval, the larger number of nodes representing intermediate contours will be added to the contour tree. This can sometimes result in a complicated multi-branch tree with an excessive length. Since our goal is to identify those critical contours representing the boundaries of the hierarchical drumlins, the contour tree can be simplified by removing those non-critical nodes. Only the critical nodes with topological changes, i.e., nodes that are immediately before merging, are kept in the simplified contour tree. Note that the root node of the tree is always preserved as it represents the maximum spatial boundary of the drumlin. Fig. 3(c) shows the simplified contour tree for the corresponding contour tree in Fig. 3(b). We can see that the compound drumlin is a level-3 drumlin with three level-1 drumlins and one level-2 drumlin nested inside. Clearly, the simplified contour tree offers a compact representation of the nested hierarchical structure of the compound drumlin.

3.3. Quantification of drumlin morphological properties

After delineating the drumlins and the nested hierarchical structure according to their topological relationships, we characterized drumlins by calculating the basic morphological properties of each drumlin, including the perimeter, area, volume, height, length (long axis), width, elongation ratio, and orientation. The perimeter and area are the circumference and area of the outermost contour of each drumlin, respectively. For example, the perimeter and area of the three level-1 drumlins shown in Fig. 3 can be derived from the three outermost contours (i.e., C, F, and K), respectively. Both the volume and height can be derived from statistical analysis of the DEM grid cells enclosed by the drumlin boundary contour. To derive length and width, we constructed the minimum bounding rectangle for each drumlin (see Fig. 4). The length and width of a drumlin are defined as the length (long axis) and width (short axis) of its fitted minimum bounding rectangle. Length and width were then used to calculate the elongation ratio (=length/width) for each drumlin.

3.4. Refinement of drumlin polygons

After computing their morphological properties, we further refined drumlins by removing those appearing to be non-drumlin features,

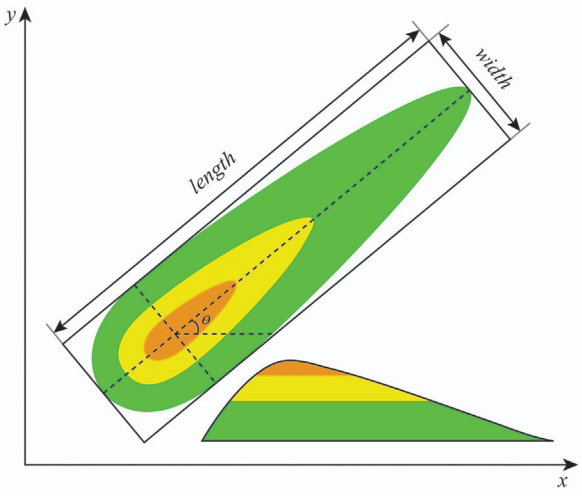

Fig. 4. Minimum bounding rectangle for a drumlin.

which were mostly human-made constructions like buildings, factories, and bridges. We set a minimum area of 5000 m^2 and a minimum height of 2 m for our study area, which were chosen based on our experimental assessment and previous studies conducted in this region (e.g., Hess and Briner, 2009; Kerr and Eyles, 2007; Maclachlan and Eyles, 2013). The criteria effectively eliminated those polygons representing small topographic undulations in low relief areas. Since drumlins vary in area, height, and shape in different parts of the world, there is no universally accepted minimum size for delineating drumlins. In addition to using area and height thresholds, manual inspection was also performed to eliminate those non-drumlin features. The remaining polygons were considered as drumlins to be used in subsequent analysis.

3.5. Implementation of drumlin extraction toolbox

To facilitate automated extraction and characterization of drumlins, the proposed methodology has been implemented as an ArcGIS toolbox – Drumlin Extraction Analyst, which can be freely downloaded at https://GISTools.github.io/#drumlin (accessed June 12, 2017). The core components of the algorithms were implemented using the open-source programming language Python. Two major Python packages being used include NumPy v1.11.3 (van der Walt et al., 2011) and ArcPy v10.4 (Esri, 2017). The Drumlin Extraction Analyst consists of three tools: DEM Preprocessing Tool, Drumlin Extraction Tool, and Drumlin Characterization Tool. The DEM Preprocessing Tool is primarily used for smoothing the LiDAR DEM using focal statistics operations, such as the mean and median filters. Each grid cell of the DEM is assigned the mean/median elevation value of all neighboring cells based on a user-specified neighborhood size. This is a recommended step for generating a smoothed DEM, which can be used as the input for all subsequent analyses. The Drumlin Extraction Tool uses the smoothed DEM as the input and executes the localized contour tree algorithm with user-specified parameters, including contour interval, base contour elevation, minimum drumlin area, and minimum drumlin height. The hierarchical drumlin polygons are saved as multiple ESRI shapefiles, each of which represents one level of drumlin polygons. The Drumlin Characterization Tool computes various morphological properties of drumlins based on the user selection. The available morphological parameters include area, volume, height, axis length, axis width, axis orientation, and elongation ratio.

3.6. Validation of drumlin extraction results

The drumlin extraction results were validated through visual and quantitative comparisons with the manual digitization method. Since the data availability of published reference maps or databases is quite limited for most of the drumlin fields, manually delineated drumlins have been widely used as the reference data to validate the automated methods (Saha et al., 2011; Yu et al., 2015). Although both manual and automated methods produce errors, checking the consistency between the drumlin mapping results through statistical measures provides a reasonable way to assess the delineation accuracy.

The manual digitization method is commonly facilitated by visualization enhancement of DEMs. Smith and Clark (2005) reviewed and tested various visualization techniques for mapping linear landforms including the drumlins. Based on their results, we mapped the drumlins of a sample site within the study area through on-screen digitizing by combining the shaded relief images and the surface derivatives. To reduce the azimuthal biases caused by different illumination angles, two shaded relief images were generated using the illuminations that are perpendicular and parallel to the principal orientation direction of drumlins. This combination of orthogonal illuminations has been demonstrated to be robust to false negatives (Smith and Clark, 2005; Yu et al., 2015). The surface derivatives including slope and curvature were used to further enhance the visualization of drumlin boundaries, which are not subject to azimuthal biases. A false color image was created by assigning the elevation, slope and curvature as red, green and blue colors. Those two shaded relief images were overlaid by the false color image whose transparency was set to 30%, and were used for subsequent manual digitization of drumlins. The manual mapping process was completed by one interpreter to minimize the inconsistency of different interpreters.

The consistency between the automated localized contour tree method and the manual digitization method was examined through visual comparisons of the drumlin mapping results and statistical comparisons of the drumlin morphological parameters. The statistical analyses were conducted for the matched overlapping drumlins both recognized by the manual method and automated method. The basic statistics including mean, standard deviation, minimum and maximum were computed for each morphological parameter. The Mann-Whitney *U* test was performed to compare the means of two drumlin datasets. The Mann-Whitney *U* test is a nonparametric statistical test to compare the differences between two independent groups. The length, width, elongation ratio, height, perimeter, and area were compared between two drumlin groups.

3.7. Characterization of drumlin spatial variation patterns

Nearest neighbor analysis and hot spot analysis were conducted to explore the spatial relationships of the drumlins and their morphological characteristics. The nearest neighbor analysis examines the spatial pattern of drumlins as dispersed, random or clustered, by measuring the distance between each feature to its closest feature and then comparing with the expected values for a random sample that follows a complete spatial randomness. This method has been used to analyze the drumlin distribution pattern in the Peterborough Drumlin Field in Ontario, Canada (Maclachlan and Eyles, 2013).

The hot spot analysis uses statistical measures to examine the spatial dependence and clustering patterns at local scales by identifying the locations of hot spots and cold spots in data. The Gi* statistic (Ord and Getis, 1995) is calculated for each feature within the context of neighboring features, and the resulting z-scores show the locations of the spatially clustered features with either high or low values. A larger positive z-score indicates more intense clustering of high values (hot spot), and a smaller negative z-score indicates more intense clustering of low values (cold spot). A statistically significant hot spot represents a high-valued feature is also surrounded by other high-valued features, and a statistically significant cold spot represents a low-valued feature is surrounded by other low-valued features as well.

The nested hierarchy is a common property of landforms generated by various Earth surface processes, such as river systems. Smaller

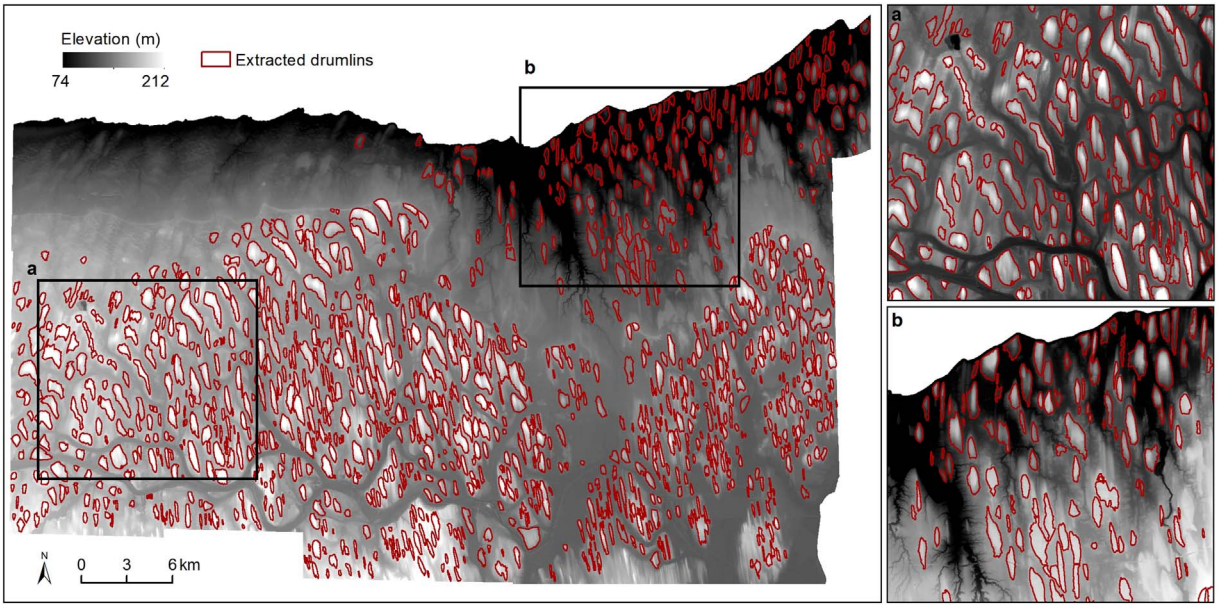

Fig. 5. Drumlin extraction results overlaid on the smoothed LiDAR DEM. a and b are the zoomed-in views of the drumlin mapping results in two regions.

landforms may be produced on top of larger ones. The contour tree representation conceptualizes the surface topography into the topological relationships between adjacent contours. The localized contour tree method represents each protruding (e.g., drumlins) or sunken (e.g., surface depressions) feature as an individual tree and retains the topological structures of those individual trees. Therefore, not only can the disjoint drumlins be extracted, but the nested topological relationships between drumlins can also be derived.

4. Results

4.1. Drumlin mapping results and accuracy assessment

Fig. 5 shows the delineation results of drumlins by using the localized contour tree method. In total, 1181 drumlins were extracted from the high-resolution LiDAR DEM for the study site. Visual assessment reveals that this automated method can successfully identify the drumlins. A sample site (Fig. 6) was selected to perform the accuracy assessment, where 194 drumlins were detected by the localized contour tree method and 144 drumlins were manually identified. This area was chosen as the sample site since drumlins of various sizes are densely distributed in this area, and the drumlins are visually distinguishable to perform the manual digitization. The manually delineated drumlins were overlaid on the automatically extracted drumlins (see Fig. 6). The visual comparison indicates that the manually mapped drumlins can be entirely identified by the automated method, while some of the drumlins extracted by the automated method were missed during the manual digitization process. Most of the matched drumlins recognized by both methods were visually consistent in shape and areal extent. Those drumlins not identified by the manual method are smaller and lower-relief forms, indicating the enhanced capability of the localized contour tree method in capturing small-scale and gentle-slope features.

The overlapping area between two drumlin extraction results is approximately 83% of the total drumlin area identified by the manual method, and 81% of the total drumlin area extracted by the automated method. The statistics of the drumlin length, width, elongation ratio, height, perimeter and area as well as the Mann-Whitney *U* test results are shown in Table 1. The statistical analyses were conducted for the matched overlapping drumlins delineated by two different methods. Table 1 shows that the mean, standard deviation, minimum, and maximum values of each morphological parameter for the matched drumlins are mostly similar, indicating the general agreement between the manual method and the automated method for extracting the majority of the drumlins. The automated method tends to produce slightly lower means than the manual method, except the width and perimeter. The automated contour tree method delineates the drumlin boundaries based on the topological relationships of the rigorously defined contours, that is, each drumlin is represented by the outermost closed-loop contour of a protruding landform. In contrast, it is difficult for the manual method to map the absolute outer boundary of the drumlins based on the shaded relief image, especially when the drumlins have quite gentle slopes. Nevertheless, the localized contour tree method is likely to merge closely spaced drumlins, resulting in larger width values than the manual method. The Mann-Whitney *U* test results indicate the significance of the differences between two drumlin groups. If the absolute value of the Z score is greater than 1.96, then the null hypothesis that two independent groups have similar means is rejected. The test results show that only height is significantly different. The similar means of the length, width, elongation ratio, perimeter and area demonstrate the consistency between the manually mapped drumlins and the automated delineated drumlins. Fig. 7 shows the comparison of each morphological parameter of the matched drumlins. The morphological properties are mostly coherent except the height. The manually mapped drumlins have higher heights than the automated delineated drumlins. These scatter plots agree well with the Mann-Whitney *U* test results.

4.2. Morphological characteristics

Based on the drumlin delineation results, the morphological characteristics of drumlins were analyzed over the study area. The minimum, maximum, mean, median, and standard deviation were computed for each morphological attribute, and the skewness and kurtosis were calculated to describe the pattern of frequency distribution. Table 2 shows the statistics on length, width, elongation ratio, height, area, and volume, and Fig. 8 illustrates the frequency histograms. The length of the extracted drumlins ranges between 101.9 m and 3494.6 m with a mean of 1011.4 m, and the width ranges between 31.2 m and 1367.2 m with a mean of 294.5 m. The average elongation ratio is 4.2 within the study area, ranging from 1.0 to 16.8. The drumlin height varies from less than 5 m to more than 50 m, and the average height is 15.9 m. The skewness is a measure of symmetry, which is zero

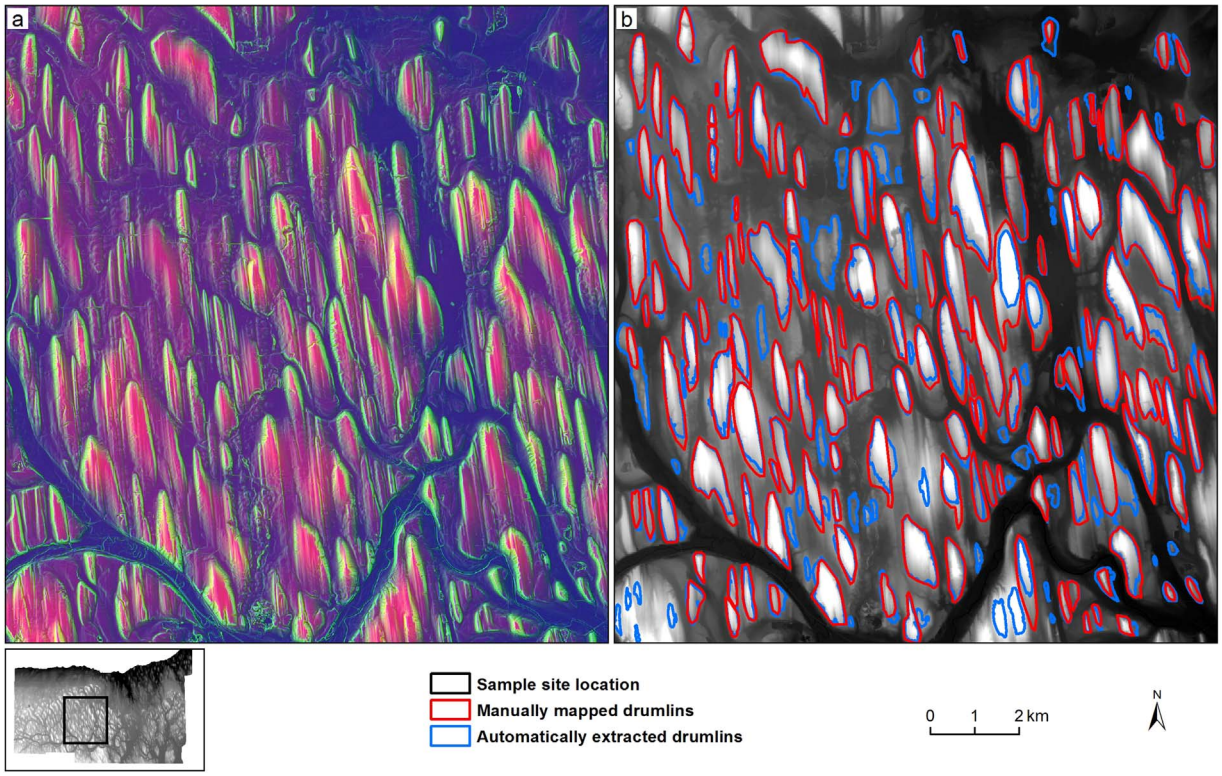

Fig. 6. The comparison between the drumlins identified by the manual mapping method and the drumlins extracted by the automated localized contour tree method. (a) Composite shaded relief image used for manual digitization (perpendicular illumination). (b) Drumlin mapping results by two methods.

for a normal distribution, positive for right-skewed data and negative for left-skewed data. Kurtosis measures whether the data are light-tailed or heavy-tailed relative to a normal distribution, which is three for a standard normal distribution, less than three for a light-tailed distribution and greater than three for a heavy-tailed distribution. The skewness and kurtosis values indicate that those six morphological parameters are notably positively skewed, and the length, elongation ratio, area and volume are heavily tailed, being consistent with Fig. 8. The area has quadratic relation with length and width, and the volume has cubic relation with length, width, and height. The frequency distributions of these two parameters are more positively skewed and heavy-tailed than other parameters, showing that drumlins occur more frequently in a smaller size but sporadically in a larger size. Akin to the drumlin fields in Britain and Ireland (Clark et al., 2009), these distributions are nearly unimodal, suggesting a single population of landforms probably formed by the same or similar processes.

The elongation ratio has a positively skewed frequency distribution pattern, varying across a wide range from nearly circular to highly elongate. As shown in Table 3, 400 drumlins (33.9%) are ovoid-shaped forms with an elongation ratio between 1 and 3, and 575 drumlins (48.7%) are moderately elongate forms with an elongation ratio between 3 and 6. The remaining 17.4% drumlins are spindle-shaped forms with an elongation ratio greater than 6, including 2.7% drumlins with elongation ratio greater than 10 that probably relate with the fast ice flows and/or ice streams of paleo-ice sheet as suggested by previous studies (Briner, 2007; Stokes and Clark, 1999).

Fig. 9(a) illustrates the relationship of drumlin width with length, showing that most of the drumlins have a length less than 1500 m and a width less than 600 m. As noted by Clark et al. (2009), the drumlins in Britain and Ireland tend to cluster at smaller sizes as well. Longer drumlins have highly variant width measurements, with elongation ratio ranging from 1 to greater than 10. Most elongate drumlins (elongation ratio > 10) have a width less than 200 m and a length greater than 500 m. The ovoid-shaped drumlins have a variety of sizes, with a width varying from 53 m to 1368 m and a length varying from 102 m to 2893 m. The drumlins with a length longer than 2000 m are mostly between ovoid-shaped and moderately elongate forms. Fig. 9(b) shows the orientation frequency of the extracted drumlins. Most of the drumlins within the study area has the long axis direction aligned north-south, with the preferred direction of 0–20° west of north.

Although the drumlin height of the study area has a wide range of 2–58 m, 88% of the drumlins are lower than 30 m, 55% of the drumlins

Table 1
The basic statistics of the drumlin morphological parameters of the manual method and the automated method and the Mann-Whitney *U* test results.

	Basic statistics								Mann-Whitney U Test	
	Mean		Standard deviation		Minimum		Maximum		Z score	Similarity
	Manual	Auto	Manual	Auto	Manual	Auto	Manual	Auto		
Length (m)	1384.5	1335.0	643.2	588.9	293.3	333.0	3125.5	3113.6	−0.526	Similar
Width (m)	307.3	316.4	181.3	177.5	48.3	68.3	1035.1	1034.9	−0.576	Similar
Elongation ratio	5.1	4.8	2.0	1.9	1.8	1.2	13.6	10.6	−1.306	Similar
Height (m)	30.4	22.2	13.1	11.6	7.2	3.9	66.1	53.1	−5.101	Different
Perimeter (m)	3015.5	3096.3	1409.1	1439.3	627.0	754.2	7293.2	7844.3	−0.425	Similar
Area (m^2)	355,925	327,038	320,167	288,395	12,488	16,096	1,619,819	1,4683,84	−0.466	Similar

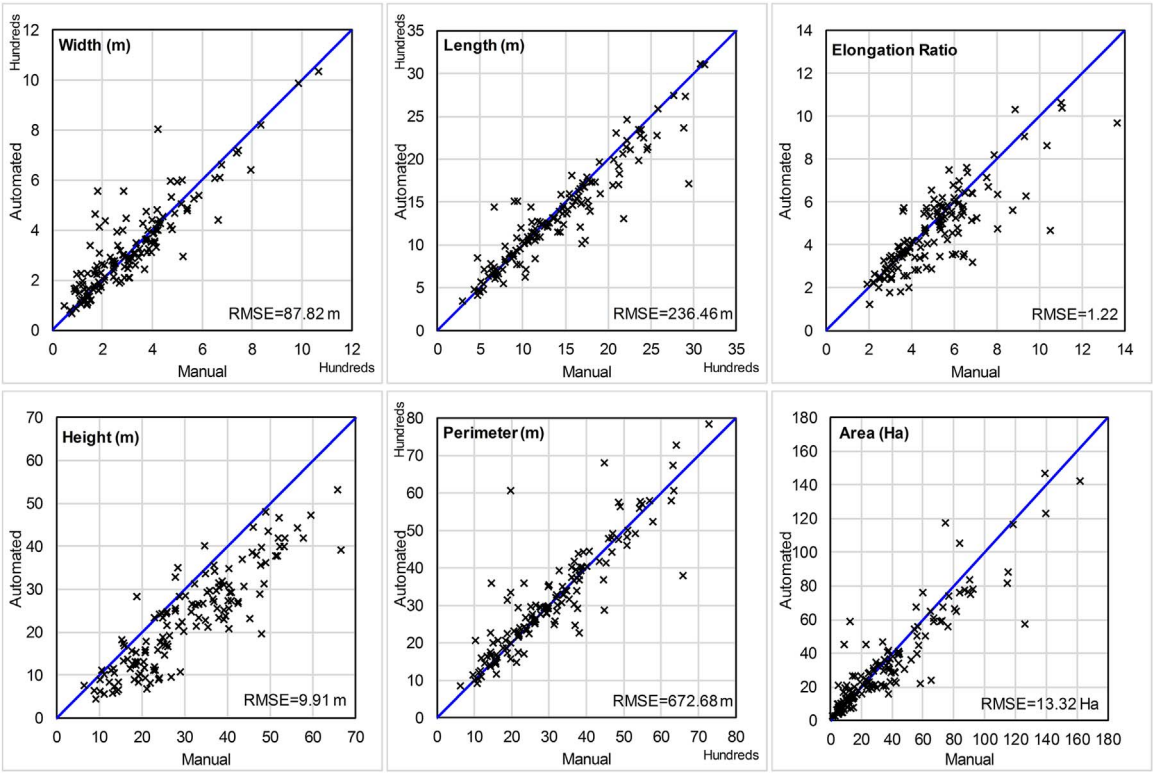

Fig. 7. Comparison of the morphological parameters between two drumlin mapping results (matched drumlins).

have a height less than 15 m, and only 3% of the drumlins are higher than 40 m. Fig. 10 shows the scatterplots of drumlin height against length, width and elongation ratio. The linearly fitting lines illustrate the positive correlations of drumlin height with length and width and the negative correlation of drumlin height with elongation ratio, yet the R^2 values are quite low. Longer or wider drumlins show more variant height values compared with shorter or narrower drumlins. The drumlins with width at lower ranges tend to increase height along with the growth of width. For the drumlins with a width less than 150 m, the majority has the height lower than 15 m. The ratio of length over height is greater than 33 for 90% drumlins, greater than 70 for 50% drumlins, and greater than 100 for 30% drumlins. The ratio of width over height is greater than 9 for 90% drumlins and greater than 19 for 50% drumlins. As for the relationship of height with elongation ratio, Fig. 10 indicates that the drumlin height decreases with the increase of elongation ratio, particularly for the highly elongate drumlins with elongation ratio larger than 10. The height of 73% spindle-shaped drumlins (elongation ratio > 6) is lower than 15 m. In contrast, the ovoid-shaped drumlins have a much wider range of height values than the elongate drumlins.

4.3. Spatial characteristics

Based on the drumlin extraction results, the nearest neighbor analysis indicates that there is a less than 1% likelihood that this clustered pattern could be the result of random chance. In other words, the drumlins within the study area exhibit significant spatial clustering patterns rather than being randomly distributed across space.

Fig. 11 illustrates the hot spot analysis results for the drumlin length, width, elongation ratio, height, area, and volume. The z-score values of −1.96 and +1.96 represent a 95% confidence level, and those of −2.58 and +2.58 represent a 99% confidence level. Fig. 11 shows that the morphological properties of width, area, and volume share similarity in spatial distribution and clustering patterns, with high values aggregating in the northwestern and the central regions of the study area, and low values aggregating in the southeastern region. In comparison with the pattern of elongation ratio, the larger-sized drumlins tend to be formed as ovoid-shaped (less elongate), while the smaller-sized drumlins have more elongate shapes. The spatial variation pattern of the elongation ratio is consistent with the previous study regarding the origin of drumlins on the floor of Lake Ontario and in upper New York State (Kerr and Eyles, 2007), which suggested that the variation in drumlin shape has clear transitions from ovoid to spindle-shaped forms and the drumlins become more elongate along the downstream flow directions of the Laurentide Ice Sheet. The drumlins in the central region have larger size both horizontally and vertically, and in contrast, those in the northeast have much shallower height.

Table 2
Statistical data describing drumlin morphological parameters.

n = 1181	Minimum	Maximum	Mean	Median	Standard deviation	Skewness	Kurtosis
Length (m)	101.9	3,494.6	1011.4	927.1	531.9	1.00	4.25
Width (m)	31.2	1,367.2	294.5	248.2	199.8	1.63	6.80
Elongation ratio	1.0	16.8	4.2	3.7	2.4	1.63	6.96
Height (m)	2.0	58.2	15.9	13.2	10.8	0.82	2.98
Area (m^2)	5112	1,848,806	236,484	155,160	253,125	2.3	10.29
Volume (m^3)	7311	23,869,597	2,150,300	858,240	3,363,058	3.0	13.89

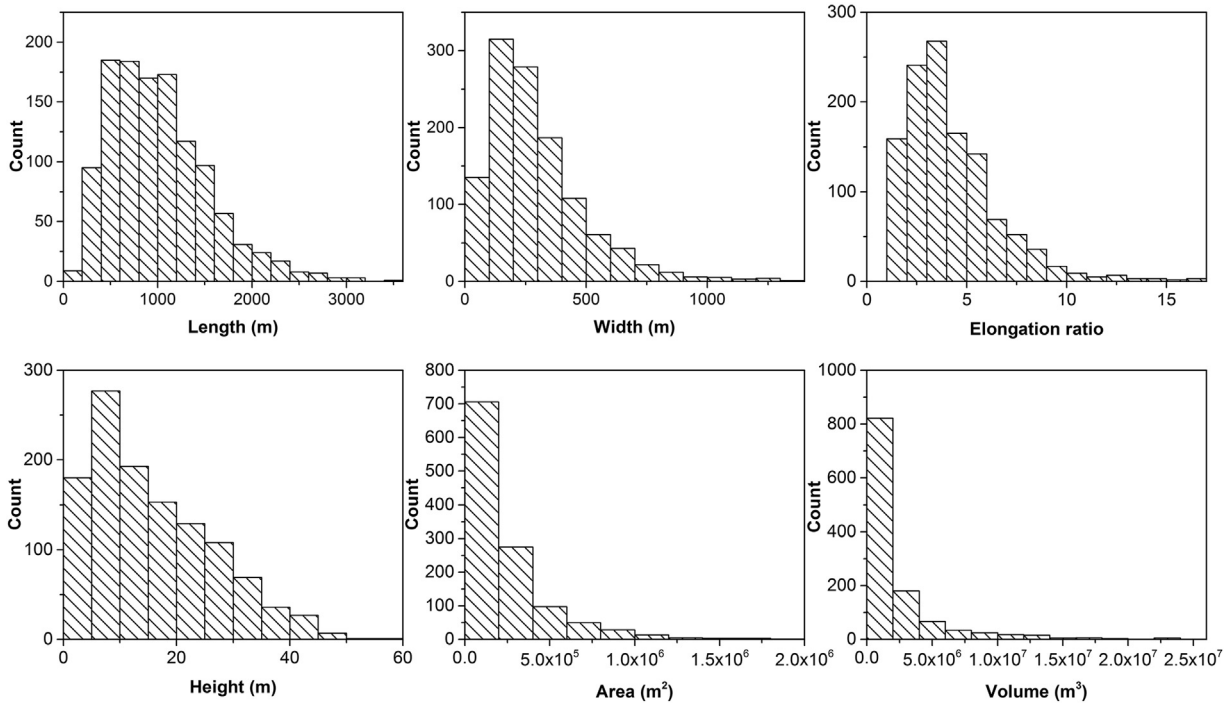

Fig. 8. Histograms of the frequency distribution of drumlin length, width, elongation ratio, height, area, and volume.

Table 3
The number and percentage of drumlins with different shapes.

Elongation ratio	Num. of drumlins	Percentage
1–3	400	33.9
3–6	575	48.7
6–10	174	14.7
> 10	32	2.7

4.4. Nested spatial structure

Fig. 12 illustrates the derivation results of the nested topological structure of the extracted individual drumlins. The boundaries of each upper level are defined by closed-loop contours as well. The lower levels merge into a single group at certain elevation height as a higher level. This nested structure can visually describe the spatial relationships between drumlins across scales. Fig. 12 shows that the drumlins in the northeastern region of the study area are much less connected comparing with the other regions. The drumlins in the central region are closely packed and aggregated into larger groups. Those drumlins merged into the same groups may have similar morphological characteristics. For example, the drumlins in the central region that are eventually grouped as Level 7 have shown significant clustering patterns in length, height, area and volume as shown in Fig. 11. Most of the merged drumlins in the southeast are spindle-shaped drumlins with smaller area and volume.

5. Discussion

This study uses a localized contour tree method to automatically identify the spatial distribution and morphological characteristics of drumlins in a portion of the New York Drumlin Field from high-resolution LiDAR topographic data. This method converts the drumlin delineation problem to the extraction of a set of concentric contours with a decreasing elevation outward from a vector-based contour map. The combination of contour tree representations and graph theory-based algorithms automates the mapping process of drumlins with high accuracy and efficiency. Compared with previous raster-based approaches, this vector-based method allows for direct derivation of the morphological and topological properties of drumlins. Besides, the

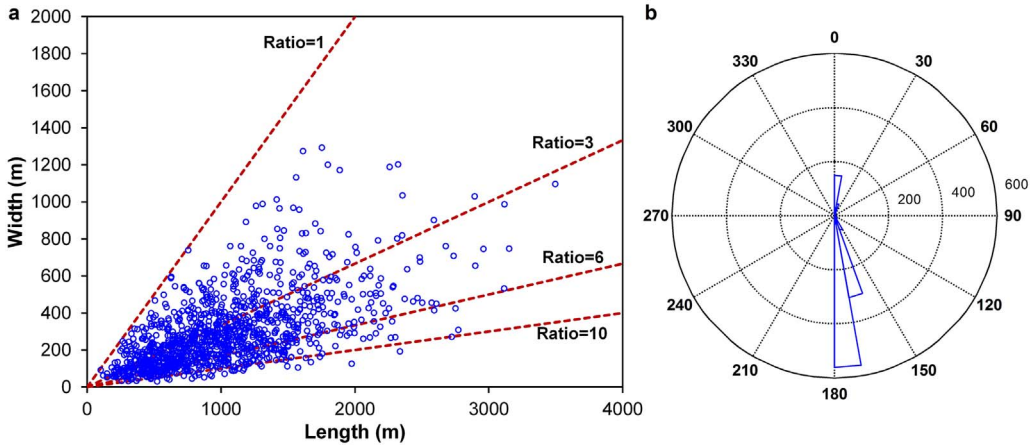

Fig. 9. (a) Drumlin width plotted against length. (b) The frequency distribution of drumlin orientation.

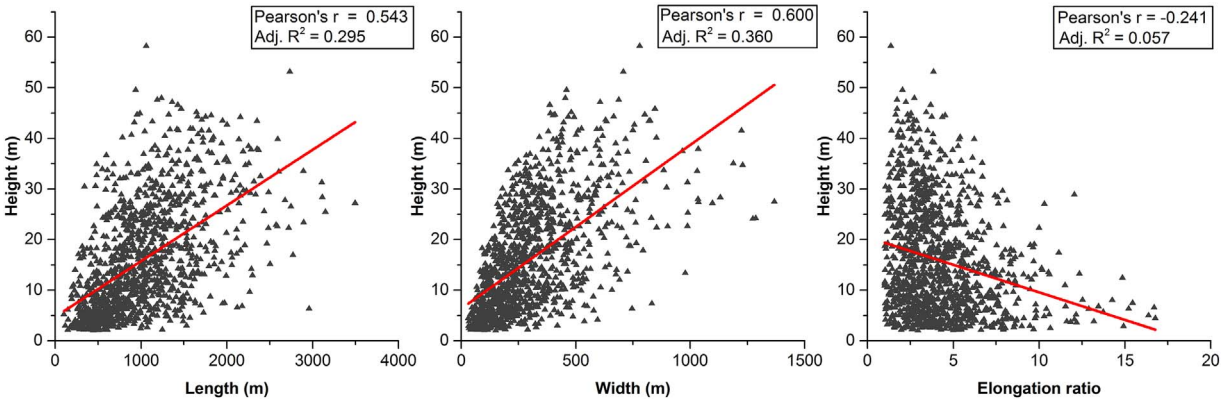

Fig. 10. Drumlin height against the length, width, and elongation ratio.

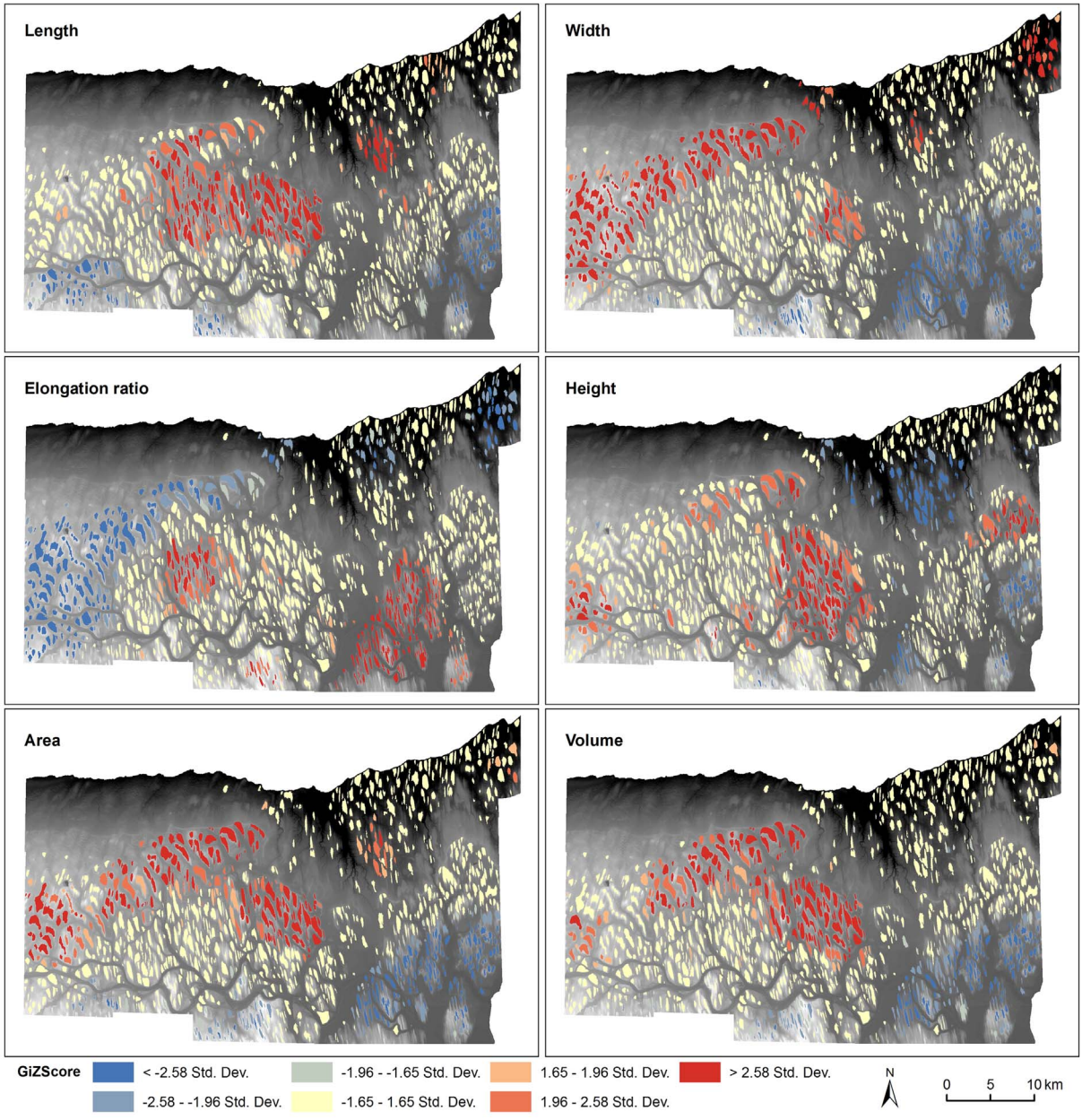

Fig. 11. Hot spot analysis results for six morphological parameters.

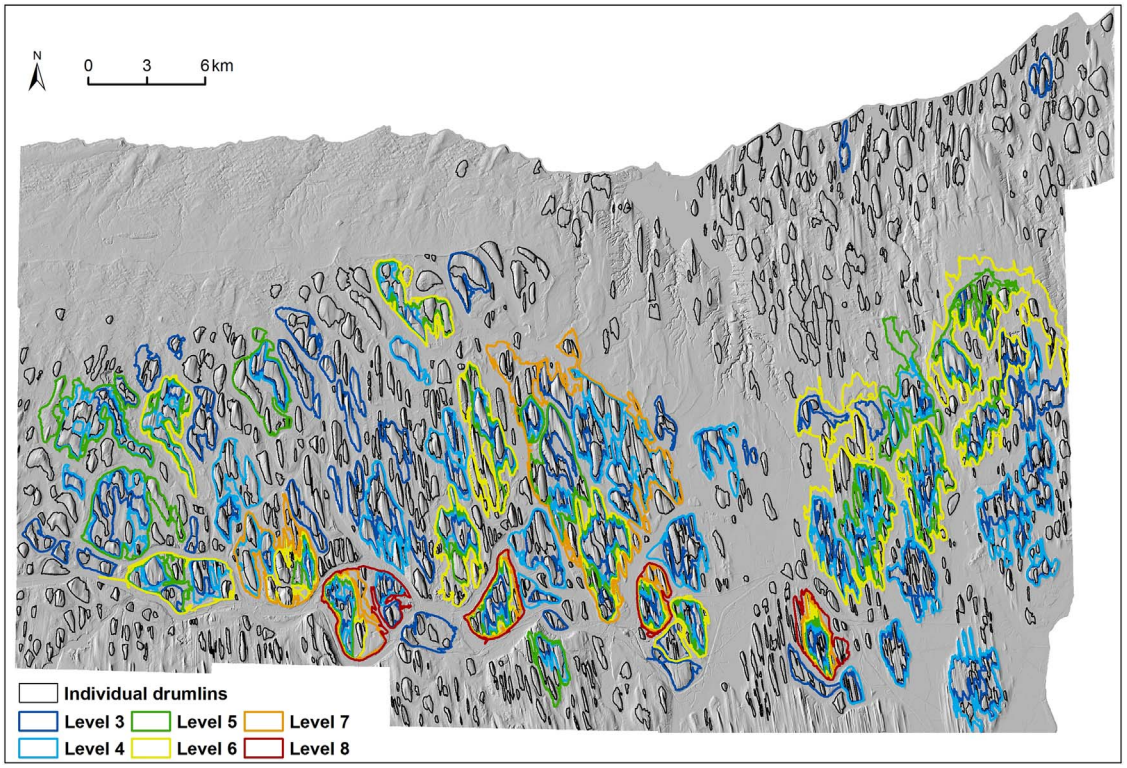

Fig. 12. The derivation results of the nested topological relationships between individual drumlins.

localized contour tree framework has the inherent advantages to describe the nested hierarchical structure of drumlins, which has gone beyond the previous drumlin mapping methods. The comparison with the manual method indicates that the drumlins extracted by our method are highly consistent with those mapped through manual interpretation of shaded relief images illuminated from different directions, and our method is able to detect smaller forms that are commonly overlooked by the manual method.

The drumlin delineation results indicate that the drumlin boundaries delimited by our automated method are smooth and comparable to the manual method. This is quite different from other automated methods for drumlin extraction. The automated object-oriented classification method developed by Saha et al. (2011) applies a multiresolution segmentation algorithm to the composite data of elevation, slope and aspect, and then classifies the irregular-shaped objects based on the manually pre-selected training samples. d'Oleire-Oltmanns et al., (2013) applied the multiresolution segmentation algorithm to merely elevation data and mapped drumlins through knowledge-based classification approach by incorporating the contextual and shape properties of segmented objects. Although the image segmentation process is fully automatic, manual selection of drumlin samples is still involved and the resulting drumlins have irregular, jagged and pixelated boundaries. As the localized contour tree method is based on the inherent topological properties of drumlins, thus manual intervention is less involved. The shadow mapping method (Pelletier, 2008) classifies the shaded relief images into shadowed and illuminated areas using predefined thresholds, and takes the doubled shadowed areas as drumlins. This method has disadvantages in deriving the accurate shapes of asymmetric drumlins, and is constrained by the azimuthal biases introduced during the generation of the shaded relief images. The relief separation method (Hiller and Smith, 2008; Yu et al., 2015) regards the residual topographic features as drumlins after removing regional topography by applying large-window median filters, which has difficulties to delineate the elongate drumlins. Our localized contour tree method is not subject to the azimuthal biases when using shaded relief images to delineate drumlins and has the capability to extract the elongate and asymmetric forms.

The reliability and accuracy of the localized contour tree method may be affected by a number of factors. As this method is based on the vector contours generated from raster DEMs, the option of the contour interval may influence the drumlin delineation results. A large contour interval would generate sparse contour lines, leading to the potential failure of detecting low-relief drumlins. In contrast, although a smaller contour interval enables the detection of low-relief drumlins, the computation complexity would be increased and more artifacts might be introduced due to noises in the DEM data. The drumlin boundaries are delimited by closed-loop contours, while the elimination of open contours may affect the delimitation of drumlins located in the areas with steep and complex topography (Yu et al., 2015). The inherent limitation of the contour-based approach is the potential underrepresentation or underestimation of the actual size of some drumlins lying upon slope, i.e., the foot-slope of a drumlin is not horizontal. This limitation is not unique to our study, as it has been reported in previous studies (Kerr and Eyles, 2007; Maclachlan and Eyles, 2013; McClenagan, 2013), which employed a similar contour-based approach to manually identify drumlins from topographic data. Nevertheless, our study area has fairly flat topographic settings, and the majority of drumlins can be delimited by closed-loop contours. The minimum area and height of the measurable drumlins are determined by the spatial resolution and vertical accuracy of the topographic data. The LiDAR DEMs used in this study have a spatial resolution of 1 m or 2 m, and the vertical accuracy of less than 15 cm (95% confidence level). The high resolution and accuracy of the LiDAR DEMs ensure the completeness and accuracy of the drumlin extraction in comparison with coarser resolution DEMs, and the localized contour tree method provides feasible and efficient solutions in dealing with LiDAR DEMs.

Quantification of drumlin size, shape and spatial patterns is important for testing a wide range of hypotheses about the drumlin formation and evolution process. The nearly unimodal frequency distributions of drumlin length, width, elongation ratio, height, area and volume suggest a single population of drumlins that were probably subject to the same or similar formation processes. As the most common

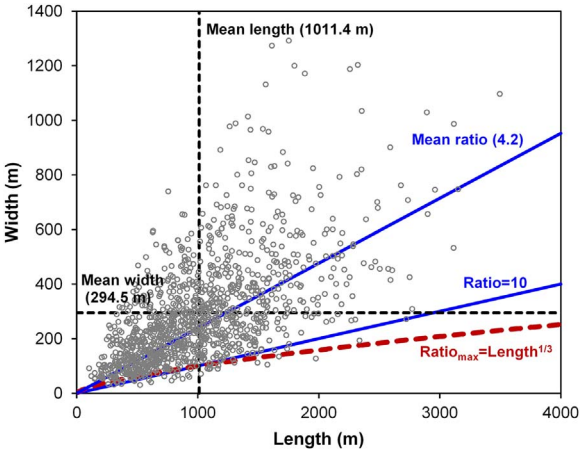

Fig. 13. The comparison between the extracted drumlins and the proposed scaling law by Clark et al. (2009).

measure of drumlin shape, elongation ratio has been used as evidence to support different theoretical hypotheses about the formation of diverse pattern of drumlin forms. It has been suggested that the elongate drumlins formed underneath the paleo Laurentide Ice Sheet related with fast ice flows (Briner, 2007; Hess and Briner, 2009). Other hypotheses to explain the elongate pattern of drumlins include the time available for drumlin formation and modification by overriding ice (Boyce and Eyles, 1991) and the thickness variations in unconsolidated sediments upon the drumlins (Kerr and Eyles, 2007). Clark et al. (2009) pointed out the importance to investigate the scaling law of drumlin shapes to test different physically-based drumlin formation models. They systematically analyzed the morphology of more than 50,000 drumlins in Great Britain and Ireland, and discovered a scale-dependent maximum elongation ratio limit (approximated by $Ratio_{max} = Length^{1/3}$). We tested this scaling law using the extracted drumlins, as illustrated in Fig. 13, showing that even though there are some outliers, the majority of drumlins conforms to this scaling law. Most of the outliers are those highly elongate forms with elongation ratio exceeding 10, some of which are probably streamlined megaflutes. The shape measures of the New York Drumlin Field in this study are consistent with their conclusion drawn from the drumlin fields in Great Britain and Ireland that there is an elongate limit for drumlins. With regard to the New York Drumlin Field, Kerr and Eyles (2007) analyzed the size and shape characteristics of 1487 drumlins within three subfields extending from the eastern half of the Lake Ontario Basin to the Finger Lakes and Onondaga Escarpment, and revealed that the drumlin morphology and spacing of the New York Drumlin Field show systematic changes, which appear to relate with the sediment thickness according to the sedimentological records of 10 coast drumlin cores. Our study area is a portion of the subfield C in Kerr and Eyles's paper. For the subfield C, they measured 978 drumlins and 60% of the drumlins are spindle-shaped to moderately elongate. Although more drumlins were extracted by using the localized contour tree method and the high-resolution LiDAR data, the morphological measures are consistent with their study, with the proportion of 66.1% of the spindle-shaped to moderately elongate drumlins and the preferred long axis direction of $0-20^{\circ}$ west of north.

The spatial pattern analysis indicates that most of the ovoid drumlins are located near the shoreline of Lake Ontario and exhibit significant clustering patterns. The highly elongate drumlins are located north of Finger Lake and Cayuga Lake in the southeast of the study area, showing the increased elongation ratio along the downstream direction of ice flows. This variation pattern is consistent with previous studies (Hess and Briner, 2009; Kerr and Eyles, 2007). Kerr and Eyles (2007) have ascribed this pattern to the difference of sediment thickness available for glacial erosion. The most elongate drumlins occur primarily in the areas of thin sediment cover. The measures of height, area and volume in this study confirm that those streamlined drumlins are attenuated forms with relatively small sediment volume. The spatial distribution pattern of drumlin forms could also be attributed to variations in ice sheet flow dynamics (Briner, 2007; Hart, 1999; Hess and Briner, 2009; Maclachlan and Eyles, 2013; Stokes and Clark, 1999). It has been hypothesized that faster moving ice tends to produce highly elongate drumlin forms, and especially those with elongation ratio greater than 10 may indicate the location of paleo-ice streams. It is plausible to explain the observed increase of elongation along downstream flowlines by the generally increased ice velocity towards ice front. Additionally, the localized contour tree method has derived the nested hierarchical structure based on the topological relationships between individual drumlins. Those drumlins merged into the same group are closely spaced and are similar in drumlin forms. This nested structure may provide new insights into the formation mechanism of drumlins and the ice flow history of the Laurentide Ice Sheet, which needs further investigations regarding the relationship of the drumlin composition and form with the nested spatial structures.

6. Conclusions

Accurate and efficient mapping and characterization of drumlins are essential for understanding and reconstructing the subglacial processes operating underneath the paleo-ice sheets. In this study, we developed an automated framework for extracting drumlins from high-resolution LiDAR DEMs using the localized contour tree method and quantifying the morphological characteristics of drumlins. It should be noted that the proposed methodology is also applicable to other DEM sources. The rationale of this method is based on the topological relationships between contours. Comparing with previous methods for mapping drumlins, this vector-based method is not affected by the azimuthal biases of shaded relief images that are commonly used for manual or automated delineation of drumlins. The elongate and asymmetric drumlin forms can be identified as well. Furthermore, this method has the capability to derive the nested hierarchical structure between individual drumlins, which may provide new insights into drumlin formation mechanism for future studies.

We applied the localized contour tree method to identify drumlins over a study area within the New York Drumlin Field, and conducted quantitative analysis of the drumlin size and form and the spatial distribution patterns of drumlins. Accuracy assessment was performed by comparing with the manual method, and the statistical comparisons show that the morphological parameters derived by the automated method are consistent with those from the manual method. The statistical analysis shows the positively skewed frequency distributions of each morphological parameter, indicating the preferred occurrence in smaller size of drumlins. The relations between length, width and elongation ratio roughly conform to the scaling law proposed by Clark et al. (2009). The drumlin distributions and morphological characteristics are not varied randomly across space, but showing significant spatial clustering patterns. The observed down-ice increases in elongation ratio are in agreement with previous studies, which may be explained by the variations in sediment thickness and/or the velocity increases of ice flows towards ice front.

Acknowledgments

This research did not receive any specific grant from funding agencies in the public, commercial, or not-for-profit sectors. The authors would like to thank the NYS ITS GIS Program Office and the Federal Emergency Management Agency for distributing the high-resolution LiDAR DEM data. The authors would like to thank three anonymous journal reviewers for providing insightful comments which improved the quality of the manuscript.

References

Argialas, D., Tzotsos, A., 2006. Automatic extraction of physiographic features and alluvial fans in Nevada, USA, from digital elevation models and satellite imagery through multiresolution segmentation and object-oriented classification. Proc. IEEE Trans. Visual. Comput. Graphics 9, 16–29.

Benn, D., Evans, D.J.A., 2014. Reader department of geography David J.A. Evans. Glaciers and Glaciation, 2nd edition. Routledge.

Boulton, G.S., Clark, C.D., 1990. A highly mobile Laurentide ice sheet revealed by satellite images of glacial lineations. Nature 346, 813.

Boyce, J.I., Eyles, N., 1991. Drumlins carved by deforming till streams below the Laurentide ice sheet. Geology 19, 787–790.

Briner, J.P., 2007. Supporting evidence from the New York drumlin field that elongate subglacial bedforms indicate fast ice flow. Boreas 36, 143–147.

Brubaker, K.M., Myers, W.L., Drohan, P.J., Miller, D.A., Boyer, E.W., 2013. The use of LiDAR terrain data in characterizing surface roughness and microtopography. Appl. Environ. Soil Sci. 2013. http://dx.doi.org/10.1155/2013/891534.

Clark, C.D., Stokes, C.R., 2001. Extent and basal characteristics of the M'Clintock channel ice stream. Quat. Int. 86, 81–101.

Clark, C.D., Hughes, A.L.C., Greenwood, S.L., Spagnolo, M., Ng, F.S.L., 2009. Size and shape characteristics of drumlinsderived from a large sample, and associated scaling laws. Quat. Sci. Rev. 28, 677–692.

Clark, C.D., 1993. Mega-scale glacial lineations and cross-cutting ice-flow landforms. Earth Surf. Processes Landforms 18, 1–29.

Clark, C.D., 1994. Large-scale ice-moulding: a discussion of genesis and glaciological significance. Sediment. Geol. 91, 253–268.

d'Oleire-Oltmanns, S., Eisank, C., Drăgut, L., Blaschke, T., 2013. An object-based workflow to extract landforms at multiple scales from two distinct data types. IEEE Geosci. Rem. Sens. Lett. 10, 947–951.

Eisank, C., Smith, M., Hillier, J., 2014. Assessment of multiresolution segmentation for delimiting drumlins in digital elevation models. Geomorphology 214, 452–464.

Esri, 2016. Minimizing Noise from Lidar for Contouring and Slope Analysis [WWW Document]. http://desktop.arcgis.com/en/arcmap/latest/manage-data/las-dataset/lidar-solutions-minimizing-noise-from-lidar-for-contouring-and-slope-analysis.htm (Accessed 06.06.17).

Esri, 2017. What Is ArcPy?—Help | ArcGIS Desktop [WWW Document]. http://desktop.arcgis.com/en/arcmap/latest/analyze/arcpy/what-is-arcpy-.htm (Accessed 06.11.17).

Evans, I.S., 2012. Geomorphometry and landform mapping: what is a landform? Geomorphology 137, 94–106.

Hart, J.K., 1999. Identifying fast ice flow from landform assemblages in the geological record: a discussion. Ann. Glaciol. 28, 59–66.

Hess, D.P., Briner, J.P., 2009. Geospatial analysis of controls on subglacial bedform morphometry in the New York Drumlin Field-implications for Laurentide Ice Sheet dynamics. Earth Surf. Processes Landforms 34, 1126.

Hiller, J.K., Smith, M., 2008. Residual relief separation: digital elevation model enhancement for geomorphological mapping. Earth Surf. Processes Landforms 33, 2266–2276.

Hindmarsh, R.C.A., 1999. Coupled ice-till dynamics and the seeding of drumlins and bedrock forms. Ann. Glaciol. 28, 221–230.

Hodge, R., Brasington, J., Richards, K., 2009. In situ characterization of grain-scale fluvial morphology using Terrestrial Laser Scanning. Earth Surf. Processes Landforms 34, 954–968.

Hughes, A.L.C., Clark, C.D., Jordan, C.J., 2010. Subglacial bedforms of the last British Ice Sheet. J. Maps 6, 543–563.

Jansson, K.N., Glasser, N.F., 2005. Using Landsat 7 ETM+ imagery and Digital Terrain Models for mapping glacial lineaments on former ice sheet beds. Int. J. Remote Sens. 26, 3931–3941.

Jennings, C.E., 2006. Terrestrial ice streams—a view from the lobe. Geomorphology 75, 100–124.

Kerr, M., Eyles, N., 2007. Origin of drumlins on the floor of Lake Ontario and in upper New York State. Sediment. Geol. 193, 7–20.

Kleman, J., Borgström, I., 1996. Reconstruction of palaeo-ice sheets: the use of geomorphological data. Earth Surf. Processes Landforms 21, 893–909.

Knight, J., 1997. Morphological and morphometric analyses of drumlin bedforms in the Omagh Basin, North Central Ireland. Geogr. Ann. Ser. A Phys. Geogr. 79, 255–266.

Li, S., MacMillan, R.A., Lobb, D.A., McConkey, B.G., Moulin, A., Fraser, W.R., 2011. Lidar DEM error analyses and topographic depression identification in a hummocky landscape in the prairie region of Canada. Geomorphology 129, 263–275.

Lindsay, J.B., 2016. Whitebox GAT: a case study in geomorphometric analysis. Comput. Geosci. 95, 75–84.

Liu, H., Wang, L., Sherman, D., Gao, Y., Wu, Q., 2010. An object-based conceptual framework and computational method for representing and analyzing coastal morphological changes. Int. J. Geogr. Inf. Sci. 24, 1015–1041.

Livingstone, S.J., Cofaigh, C.Ó., Evans, D.J.A., 2008. Glacial geomorphology of the central sector of the last British-Irish Ice Sheet. J. Maps 4, 358–377.

Lu, P., Stumpf, A., Kerle, N., Casagli, N., 2011. Object-oriented change detection for landslide rapid mapping. IEEE Geosci. Rem. Sens. Lett. 8, 701–705.

Maclachlan, J.C., Eyles, C.H., 2013. Quantitative geomorphological analysis of drumlins in the Peterborough drumlin field Ontario, Canada. Geogr. Ann. Ser. A. Phys. Geogr. 95, 125–144.

Martha, T.R., Kerle, N., Jetten, V., van Westen, C.J., Kumar, K.V., 2010. Characterising spectral, spatial and morphometric properties of landslides for semi-automatic detection using object-oriented methods. Geomorphology 116, 24–36.

McCABE, A.M., Knight, J., McCARRON, S.G., 1999. Ice-flow stages and glacial bedforms in north central Ireland: a record of rapid environmental change during the last glacial termination. J. Geol. Soc. London 156, 63–72.

McClenagan, J.D., 2013. Streamlined erosional residuals and drumlins in central British Columbia, Canada. Geomorphology 189, 41–54.

Menzies, J., 1979. A review of the literature on the formation and location of drumlins. Earth-Sci. Rev. 14, 315–359.

Notebaert, B., Verstraeten, G., Govers, G., Poesen, J., 2009. Qualitative and quantitative applications of LiDAR imagery in fluvial geomorphology. Earth Surf. Processes Landforms 34, 217–231.

Ord, J.K., Getis, A., 1995. Local spatial autocorrelation statistics: distributional issues and an application. Geogr. Anal. 27, 286–306.

Pelletier, J.D., 2008. Quantitative Modeling of Earth Surface Processes. Cambridge University Press, Cambridge.

Rose, J., Letzer, J.M., 1977. Superimposed drumlinsm. J. Glaciol. 18, 471–480.

Saha, K., Wells, N.A., Munro-Stasiuk, M., 2011. An object-oriented approach to automated landform mapping:A case study of drumlins. Comput. Geosci. 37, 1324–1336.

Seneca NY Watershed LiDAR Control, 2014. https://gis.ny.gov/elevation/metadata/Seneca-NY-Watershed-LiDAR-Control.xml (Accessed 17.05.30)

Shaw, J., Freschauf, R.C., 1973. A kinematic discussion of the formation of glacial flutings. Canad. Geogr./Le Géographe Canadien 17, 19–35.

Shaw, J., 1983. Drumlin formation related to inverted melt-water erosional marks. J. Glaciol. 29, 461–479.

Shaw, J., 1989. Drumlins, subglacial meltwater floods, and ocean responses. Geology 17, 853–856.

Smith, M.J., Clark, C.D., 2005. Methods for the visualization of digital elevation models for landform mapping. Earth Surf. Processes Landforms 30, 885–900.

Smith, M.J., Rose, J., Gousie, M.B., 2009. The Cookie Cutter: a method for obtaining a quantitative 3D description of glacial bedforms. Geomorphology 108, 209–218.

Spagnolo, M., Clark, C.D., Hughes, A.L.C., 2012. Drumlin relief. Geomorphology 153–154, 179–191.

Stokes, C.R., Clark, C.D., 1999. Geomorphological criteria for identifying Pleistocene ice streams. Ann. Glaciol. 28, 67–74.

Stokes, C.R., 2002. Identification and mapping of palaeo-ice stream geomorphology from satellite imagery: implications for ice stream functioning and ice sheet dynamics. Int. J. Remote Sens. 23, 1557–1563.

United States Interagency Elevation Inventory, 2016. https://coast.noaa.gov/inventory/ (Accessed 02.01.17).

van der Walt, S., Chris Colbert, S., Varoquaux, G., 2011. The NumPy array: a structure for efficient numerical computation. Comput. Sci. Eng. 13 (2), 22–30 (arXiv [cs. MS]).

Wu, Q., Lane, C.R., 2016. Delineation and quantification of wetland depressions in the prairie pothole region of north dakota. Wetlands 36, 215–227.

Wu, Q., Lane, C.R., 2017. Delineating wetland catchments and modeling hydrologic connectivity using LiDAR data and aerial imagery. Hydrol. Earth Syst. Sci. Discuss. 1–32.

Wu, Q., Lane, C., Liu, H., 2014. An effective method for detecting potential woodland vernal pools using high-resolution LiDAR data and aerial imagery. Remote Sens. 6, 11444–11467.

Wu, Q., Liu, H., Wang, S., Yu, B., Beck, R., Hinkel, K., 2015. A localized contour tree method for deriving geometric and topological properties of complex surface depressions based on high-resolution topographical data. Int. J. Geogr. Inf. Sci. 29, 2041–2060.

Wu, Q., Deng, C., Chen, Z., 2016. Automated delineation of karst sinkholes from LiDAR-derived digital elevation models. Geomorphology 266, 1–10.

Yu, P., Eyles, N., Sookhan, S., 2015. Automated drumlin shape and volume estimation using high resolution LiDAR imagery (Curvature Based Relief Separation): a test from the Wadena Drumlin Field, Minnesota. Geomorphology 246, 589–601.